Available online at www.CivileJournal.org

Civil Engineering Journal

(E-ISSN: 2476-3055; ISSN: 2676-6957)

Vol. 11, No. 02, February, 2025

The Effect of Additional Baffle Plates on Double-Stage Gravitational Water Vortex Turbine

Ari Prasetyo [1*], Eki Rovianto [1], Dimas Adika [1], Reza Maulana [2], Muhamad D. Septiyanto [2], Eko P. Budiana [2], Syamsul Hadi [2], Dandun M. Prabowoputra [3]

[1] *Department of Mechanical Engineering, Vocational School, Universitas Sebelas Maret, Surakarta 57126, Indonesia.*

[2] *Department of Mechanical Engineering, Universitas Sebelas Maret, Surakarta 57126, Indonesia.*

[3] *Department of Mechanical Engineering, Universitas Jendral Soedirman, Purbalingga, Indonesia.*

Received 25 October 2024; Revised 18 January 2025; Accepted 23 January 2025; Published 01 February 2025

Abstract

A Gravitational Vortex Water Turbine (GWVT) is an appropriate device to harness the kinetic energy of water to convert it into rotational mechanical energy in low-head. The water flow is directed into a circular basin, which can produce a vortex and can rotate the turbine blades. Turbine performance is influenced by the shape of the blade, so an optimal blade shape is required. Turbine performance is influenced by the shape of the blades, which can rotate optimally. This study aims to determine the effect of adding baffle plates in the blade on the performance of two-stage GWVT using experimental methods. The variation used is the proportion of baffle plate on the runner in the first stage with variations without baffle plate, 25%, 50%, 75%, and 100%. The data taken in the test is the torque and rotation at each additional blade plate. Torque measurement uses a rope brake system, and rotation measurement uses a tachometer. The results of the study showed that the addition of a 50% baffle plate in the first stage can capture the energy of the water vortex more optimally. A baffle plate can increase efficiency by up to 23.15% compared to the blade without the addition of a baffle plate.

Keywords: Vortex Turbine; Baffle Plate; Double Stage; Performance.

1. Introduction

Indonesia has a target of providing renewable energy as a source of electricity of 31% by 2050 and zero emissions by 2060 [1]. Hydropower is a sustainable energy option used for years, with the working principle of converting kinetic energy into electricity [2, 3]. This environmentally friendly resource has various advantages, including its cleanliness, affordability, and positive impact on environmental ecology [4]. It is especially important for areas with hills or proximity to rivers and lakes that have a vital role in ensuring a sustainable future [5-7]. The use of hydropower as a renewable energy source is highly recommended for academic studies related to water management and sustainable development [8, 9]. Vortex turbines are innovative devices that harness the power of vortex water to generate electricity [10, 11]. The use of vortex turbines offers a sustainable and efficient solution for generating clean energy from low-head water sources [12, 13]. The use of vortex flow was first initiated by Viktor Schauberger, but research on GWVT began to be glimpsed by the world after Zotloter used it in the Obergrafendor River, Austria, which can produce a power of 10 kW in 2006 [14]. The advantage of the vortex turbine is that it can operate without a dam and can operate on river flows with a small flow rate [15].

* Corresponding author: ari_prasetyo@staff.un.ac.id

http://dx.doi.org/10.28991/CEJ-2025-011-02-011

Various studies have been carried out to improve the performance of water turbines in optimizing the potential available in an area [16, 17]. The configuration design of the Vortex turbine plays a crucial role in maximizing its efficiency [18]. Other parameters on vortex turbines, such as inlet velocity, basin shape, basin height [19], and mass flow rate [20], the efficiency of the vortex turbine can be significantly influenced [21, 22]. Many of these have highlighted the need for more research on this topic due to the improvements in vortex turbine technology [23]. Additionally, the applicability of smart vortex turbines that incorporate a motor in the form of a generator has been established to harness electrical energy from mechanical power attained from a water vortex [24]. This makes the number of blades become a parameter that influences the performance and efficiency of a vortex turbine [25, 26]. The efficiency of the water turbine is known to be positively affected by a rise in the number of blades used; this normally results in a direct relation between the number of blades and the torque produced [27]. This is because the blade is made up of a larger surface area, and therefore more blades mean that the water can exert more force on the blades, hence transferring more kinetic energy to rotational energy [28]. The choice of a specific configuration of blades for a vortex turbine significantly defines its parameters, efficiency, and performance [29]. The use of the profile of the blade defines the flow dynamics and interaction with the vortex leading to the effects on the efficiency and performance of the turbine [30]. Contrary to assumptions about the shape of blades, the flow of the vortex and the abilities of the turbine to use the energy within the vortex can differ [31]. It is also necessary to note that the specifics of the formation and stabilization of vortices in a turbine are realized concerning detailed characteristics of the blade profile, dimensions, and curvature [32].

Blade profiling with higher curvature and generally more compact shapes produces stronger vortices that improve energy conversion efficiency. In addition, the aspect ratio and inclination of the blades are crucial in deciding the effectiveness of the vortex turbine [33]. Various essential parameters define the performance of a two-stage vortex turbine. Such factors involve the efficiency of the turbine under partial load [34]. The performance of the turbine is also greatly influenced by design parameters, which include the rotor ratio, offset distance between neighboring runners, and intra- and inter-staging configurations of the turbine. Also, the profile of the blades of upstream runners alters the vortex distortion and therefore influences the power capacity of downstream runners [34-36]. To get a deeper insight into the operating principles of a two-stage vortex turbine and to obtain maximum efficiency, detailed theoretical and experimental studies are indeed required from the previous analysis. These investigation details should include examining the influence of design parameters [37, 38], load conditions [39], and blade profiles [39, 40] on rotational speed, torque [41], and power turbine [42].

Sritram & Suntivarakorn [43] conducted a study on the effect of the number of spoons used on GWVT. They conducted trials with different numbers of spoons. As a result, a turbine that uses 5 blades produces the maximum torque value and efficiency. Sritram et al. [11] also conducted experiments on the effect of additional baffle plates with a proportion of 50% area on turbine blades. Based on research conducted by Sritram et al. [11], the addition of a baffle plate can increase the torque and efficiency of the turbine. Previous research about baffles was conducted by Wichian et al., who tested the effect of adding baffle plates to water turbines to improve the performance of GWVT using the CFD method. Wichian et al. used a runner with a diameter of 45 cm, a height of 32 cm, and several blades of 5 blades. This test simulates with several variations, namely runners without the addition of baffle plates, and additions with an area proportion of 0%, 25%, 50%, 75%, and 100%. As a result of the simulation carried out, the most optimal addition of baffle plates is the proportion of 50% area. Runners with an additional 50% baffle plate have the highest torque value of 37.41 Nm, and efficiency reaches 32.79% higher than runners that do not use an additional baffle plate [44]. Modifying the blade in each type of turbine has been proven in various studies to improve performance [45, 46]. In 2015, Jeon et al. [47] conducted a study on the effect of baffle plate size on Savonius wind turbines. As a result of the research conducted, the baffle plate was able to increase the power coefficient (Cp) and torque coefficient (Ct) [47]. Another study related to the function of the baffle plate was conducted by Kassab et al. [48] who examined the baffle plate effect on Savonius turbine with the CFD method. The study showed the baffle plate serves to direct the flow of wind that propels the turbine so that it can increase power and torque.

This study fills the research gap on vortex turbine configurations. Firstly, the velocity distribution in the vortex flow inside the conical basin has been revealed in the study of Dhakal et al. [12]. Another supporting research is the use of a baffle plate in a single-stage vortex turbine that can increase turbine efficiency [44]. Based on this literature, it is necessary to develop the use of a baffle plate configuration to optimize the fluid velocity distribution within the conical basin with a double-stage vortex turbine configuration. Moreover, the lower turbine utilizes the additional baffle plate configuration to harness the co-axial vortex flow after the upper turbine impacts. To see the effect of adding the best baffle plate, this study will examine the variation in the proportion of baffle plates that increase maximum performance for the GWVT double stage. The variations used are spoons without baffle plates; the proportion of baffle plates is 25%, 50%, 75%, and 100%.

2. Experiment Method

2.1. Blade Design

The curvature of the blade is chosen to obtain optimal efficiency. Previous studies have concluded that blade curvature influences turbine performance. In this study, a curvature of 35° and 5 blades were used in the first stage [11]. Dhakal et al. state that the curvature of the turbine blade affects efficiency [49]. Septyaningrum et al. [50] study that a runner with 5 blades is the optimal number for a double-stage turbine that generates the highest mechanical power and efficiency. Figure 1 provides details of the blade design utilized in this investigation.

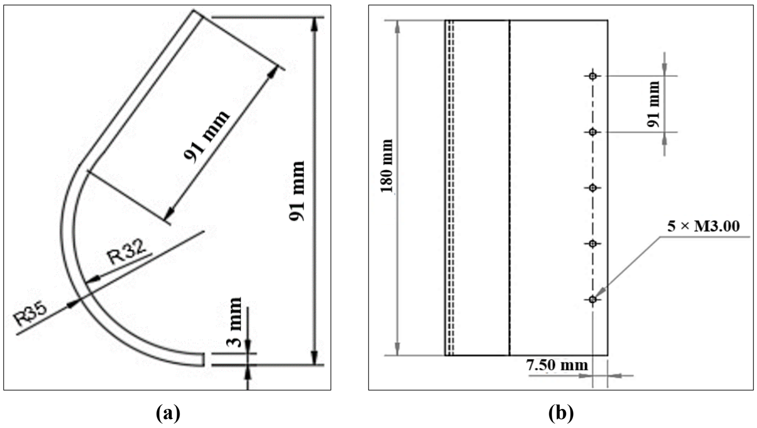

Figure 1. (a) Curvature (b) Size blade

The stage-2 turbine design has an inclination angle that has the same configuration in all this experimental set-up. According to Handoko et al., the inclined turbine has a relatively good receiving amount of momentum water, which has an angle when rotating within the basin [16]. Physically, when the turbine has the same inclination to the vortex angle, flow can harness superior power output and systems efficiency. The stage-2 turbine dimension is provided in Table 1.

Table 1. Runner Stage 2 Geometry

Parameters	Value
Inlet angle	30°
Outlet angle	45°
Radius of curvature	35 mm
Blade width	90 mm
Blade height	180 mm
Thickness	2 mm
Blade number	5
Hub diameter	120 mm
Turbine material	Aluminium

The additional baffle is installed at the stage-1 turbine, which has a possible enhancement in efficiency and power output that was considered in the previous single-stage vortex turbine conducted by Sritram & Suntivarakorn [43]. Related to his findings, a 50% baffle proportion with top and bottom baffles generated the highest efficiency, 43.83%. In this context, the additional baffle results in more catching momentum that leads the efficiency to be higher. The study examined variations of the runner design with and without baffles in a double-stage vortex turbine configuration, using 25%, 50%, 75%, and 100% baffle proportions, as shown in Figure 2.

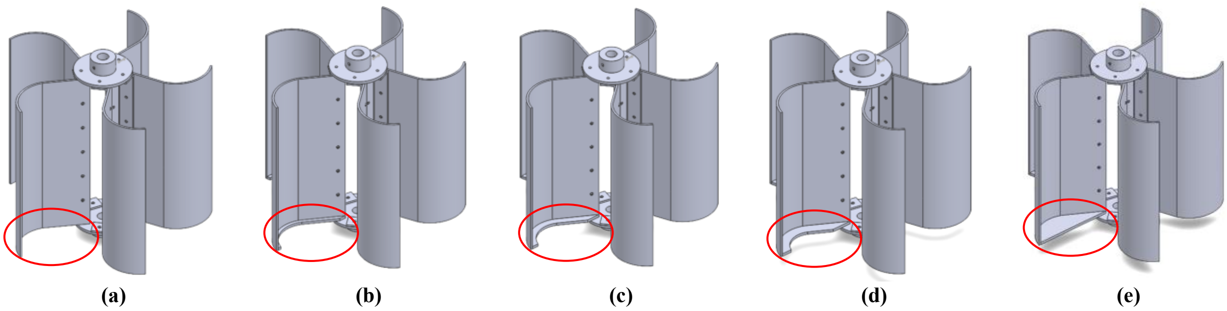

Figure 2. Baffle Plate Runner (a) without, (b) 25%, (c) 50%, (d) 75%. (e) 100%

2.2. Apparatus Test

The experimental device used during the test was a low-speed water tunnel to form sufficient low head. That water tunnel constructed from steel has dimensions of 2.2 meters in width, 1.9 meters in height, and 4.4 meters in length, with a capacity of 1 cubic meter in the bottom reservoir. Its device was designed to get low speed and natural vortex with uniform flow. The study selected a conical basin for its superior performance over a cylindrical basin [51]. Figure 3 shows the apparatus test and conical basin dimension used in this study.

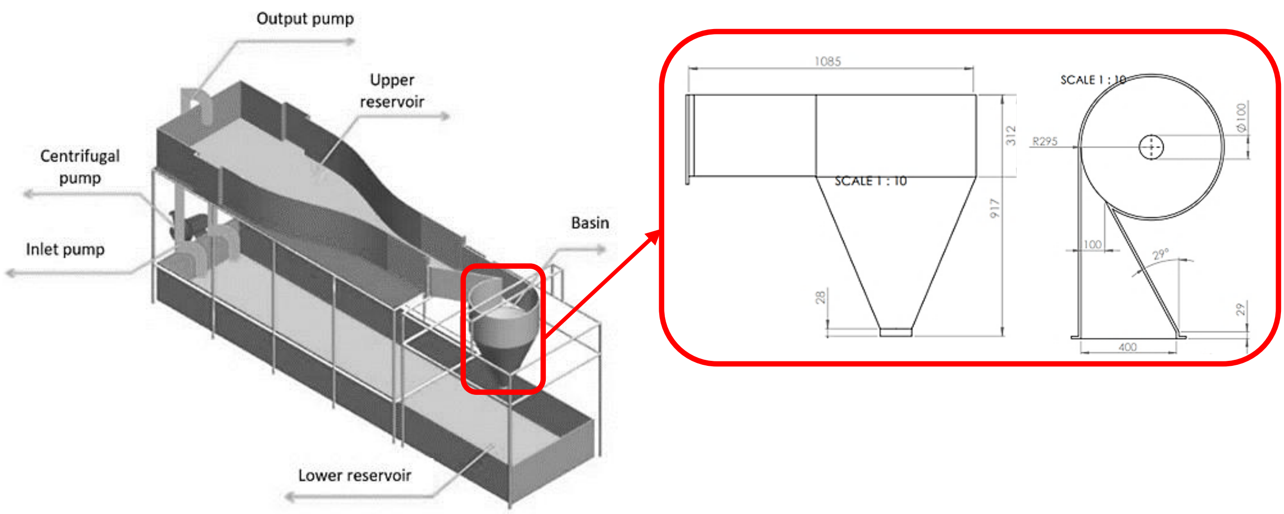

Figure 3. Low-speed water tunnel and conical basin design

The parts and functions of the testing tool are as follows:

- The lower reservoir functioned as the water accommodation chamber.
- The inlet pipeline in centrifugal pumps functioned as a suction channel for transferring water to the upper channel.
- The centrifugal pump is used for continuously pumping the water from the bottom to the upper tunnel.
- The outlet pipe is a channel for exiting water transferring from the bottom tunnel.
- A honeycomb located in the upper reservoir closed with the outer transferring pipe has the functionality to stabilize the water.
- The upper tunnel has the functionality to collect the entering water from the bottom tunnel and guide it to the conical basin.
- The basin is designed in a conical shape with different inlets and outlets to generate a natural vortex flow.

The low-speed water tunnel operates on the principle of creating a vortex flow within a conical basin. The water from the bottom tunnel is pumped to the upper tunnel using a centrifugal pump. Water that exists at the outlet flows through the upper tunnel and the honeycomb. It must be considered that the honeycomb has the functionality to reduce the wave and streamline the flow with constant height in the upper tunnel. After that, the water gradually flows to the conical basin and forms a vortex flow, which is harnessed by the turbine. This experiment uses a constant flow rate of 9.5 l/s, conditioned with the bypass valve channel. To ensure the continuous flow rate, we use ultrasonic flow meter sticks on the outer surface of the exit pipe. The definitions of blade position were presented in stage-1 (bottom turbine) and stage-2 (upper turbine). Considering the distance between each turbine, it becomes critical to consider that it also influences the turbine's performance. The very close distance between the two stages creates a destructive flow, reducing the turbine's ability to harness the energy. According to research conducted by Sinaga et al. (2023) [51], the optimal distance between the first and second stages, which minimizes vortex distortion caused by the second-stage runner and maximizes flow energy conversion, is 10 cm, as presented in Figure 4-a.

The torque measured by using a rope brake system is shown in Figure 4-b. The load on stage 1 is varied between 1-1.75 kg, while the load on stage 2 is kept constant at 1 kg. The load is varied to analyze the mechanical power and efficiency generated under different rotations, as shown in Table 2. The turbine rotation speed is measured on the turbine shaft using the tachometer. We took measurements under steady flow conditions and repeated those three times to achieve more accurate results. Measurements were taken when the flow conditions were steady and repeated three times to get more accurate results. Figure 5 is the flow chart of the experimental procedure.

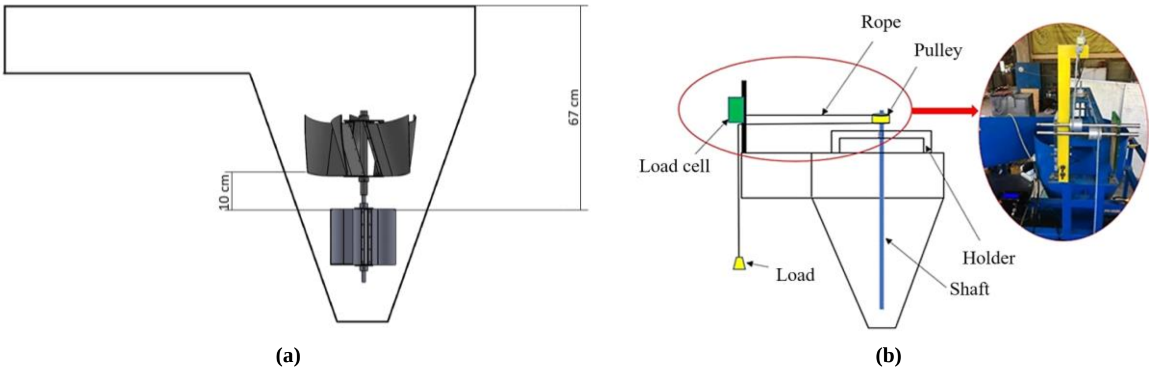

Figure 4. (a) Runner Position, (b) Rope Brake System [52]

Table 2. Test load variations

Load on stage 1 (kg)	Load on stage 2 (kg)
0.75	1.00
1.00	1.00
1.25	1.00
1.50	1.00
1.75	1.00

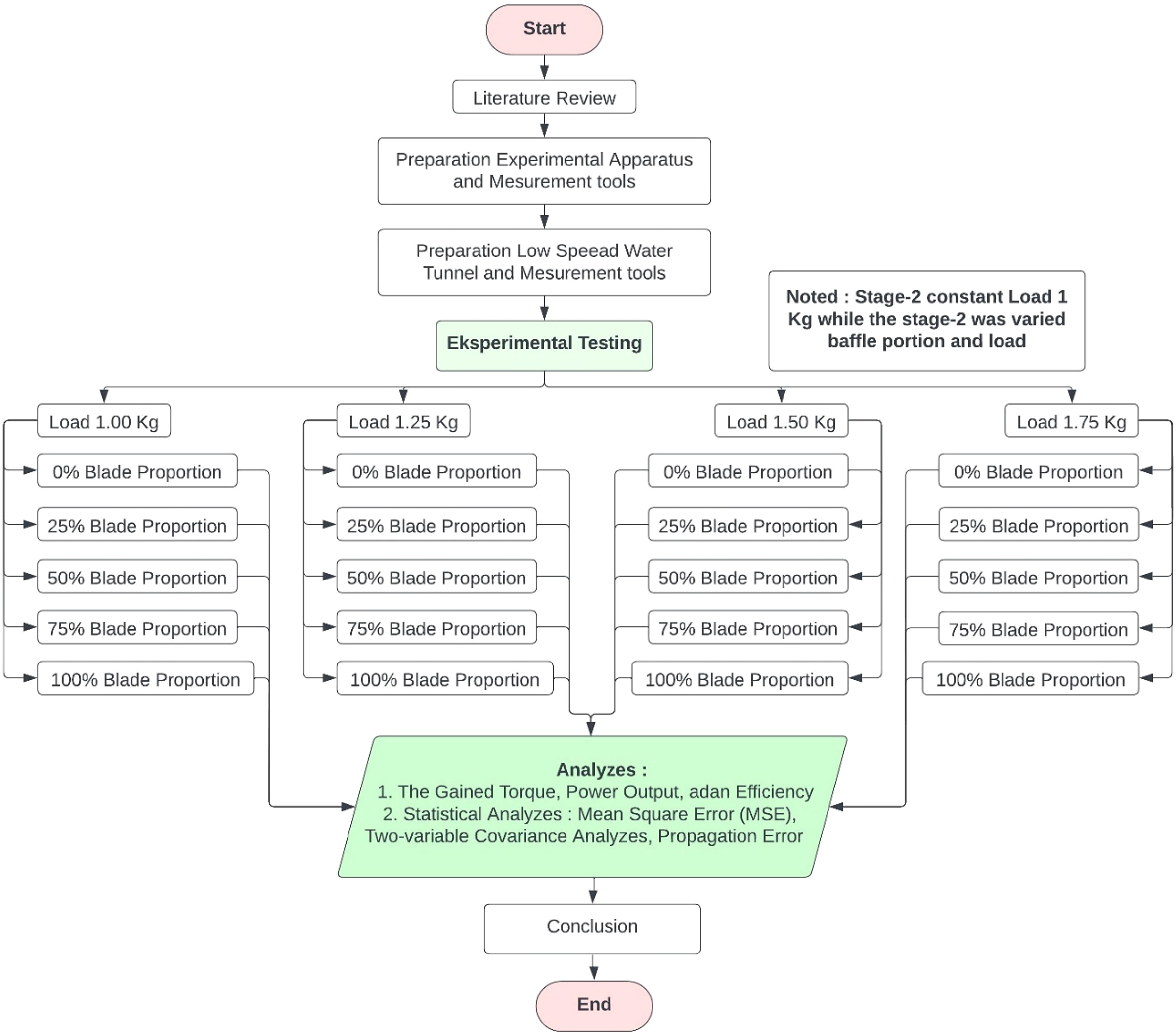

Figure 5. Flow Chart of the methodology

2.3. Equation

The input power is power stored by flowing fluid that generates a turbine [21].

$$P_{in} = \rho g Q H_v \tag{1}$$

where ρ is density of water (1000 kg/m^3), g is acceleration gravity (9.81 m/s^2), Q is water flow rate (m^3/s), dan H_v is vortex height (m).

The mechanical torque of a turbine can be defined by (*T*) is calculated by the following equations.

$$T = Fr \tag{2}$$

The rotational speed of the turbine defined by (ω) can be calculated by the following equations:

$$\omega = \frac{2\pi N}{60} \tag{3}$$

The turbine mechanical power is generated by the rotation speed and torque of the shaft. It can be calculated as:

$$P_m = T\omega \tag{4}$$

Efficiency describes the performance of variations in adding buffer plates. The magnitude of this value results from the comparison of mechanical power with input power which can be calculated by the following equations.

$$\eta = \frac{P_m}{P_{In}} \times 100\% \tag{5}$$

3. Result and Discussion

3.1. Torque

Torque is one of the parameters for evaluating turbine performance. It represents the rotational force generated by the turbine, which allows for the measurement of power and the turbine's ability to convert fluid flow energy into mechanical energy. The generated torque can be calculated by multiplying the braking force/load (F) from the rope brake system by the radius or pulley radius (r) [21].

Figure 6 shows the torque values for different baffle proportions in stage 1. The 50% baffle proportion achieves the highest torque at a load of 1.75 kg, with values of 0.71 Nm at 168 rpm and 0.46 Nm at 210 rpm under a 1 kg load. Baffles with 25%, 75%, and 100% proportions yield larger torques compared to a turbine without baffle plates, with respective peak values of 0.62 Nm at 160 rpm, 0.70 Nm at 150 rpm, and 0.66 Nm at 145 rpm. These results indicate that the addition of baffle plates can hold more water, thus increasing the amount of water that hits the turbine blades. The turbine with a 50% baffle produces the highest torque because it can hold the water that hits the blades. Additionally, the co-axial flow vortex after hitting stage-2 is maximally harnessed by the baffle plate in stage-1. At a load of 1.75 kg, turbines with 75% and 100% baffles exhibit unstable rotation, while the 50% baffle is more stable. Therefore, the 50% baffle turbine achieves the maximum torque. On the other hand, the turbine without baffles has the least torque, with a maximum value of only 0.6 Nm at 155 rpm. This shows that adding a baffle plate can increase torque, with a maximum increase of 18% at a 50% baffle proportion.

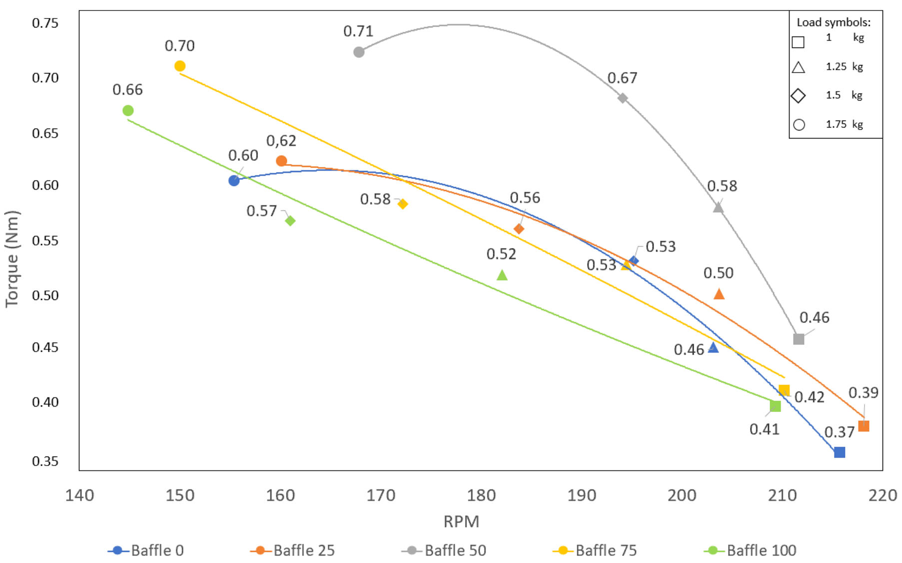

Figure 6. Stage 1 Torque

The turbine's performance between stage 1 and stage 2 influences each other. That statement is strengthened by Figure 7, where stage 2 has the same geometry, but the torque is gained differently under the varied baffle portions in stage 1. However, this significant effect of baffle in Stage 1 to Stage 2 is not revealed in all variations; for example, the torque produced in Stage 2 when Stage 1 is using no baffles, 25%, 50%, or 75% baffles has the same value of 0.28 Nm. On the other hand, when it uses a 100% baffle, the value is slightly higher at 0.29 Nm. The same condition has also been observed in their rotational speed, which is 135 rpm in Stage 2 under 25%, 50%, or 75% baffle portions in Stage 1, compared to 132 rpm for the 100% baffle plate. The best performance was generally generated by 50% baffle with 0.46 Nm at 114 Nm. There is a significant difference in torque and rpm results when stage 2 is paired with a 75% baffle variation and a 100% under starting load of 1.25 kg. This significant difference in torque and rpm is due to the vortex height being greatly reduced when the load is 1.25 kg, resulting in less water hitting the blades at stage 2.

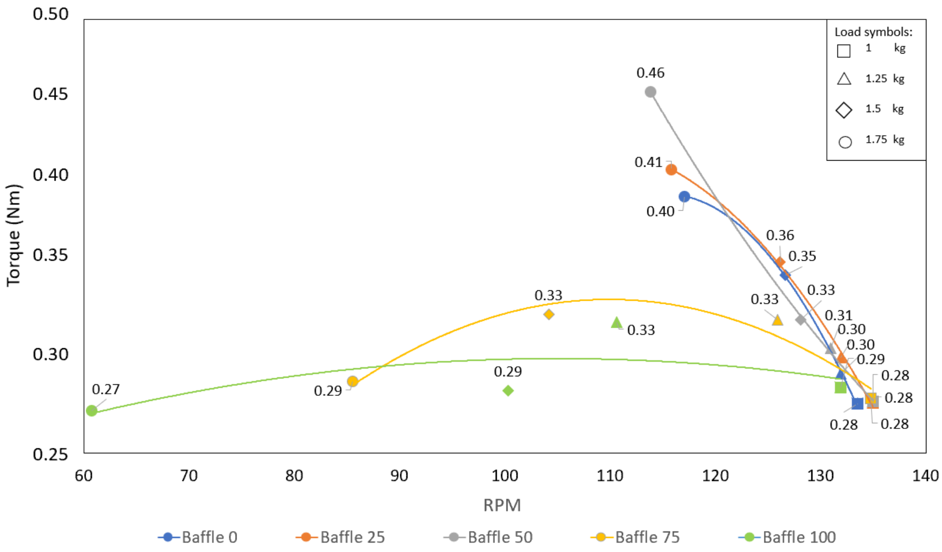

Figure 7. Stage 2 Torque

3.2. Mechanical Power

Mechanical power is measured by multiplying the turbine's torque and angular velocity. This calculation represents how much fluid flow energy is converted into mechanical energy, so mechanical power is the fundamental parameter used to measure how optimally a turbine works.

Figure 8 shows the results of experiments conducted with 4 load variations: 1 kg, 1.25 kg, 1.5 kg, and 1.75 kg. The turbine with a 50% baffle produces a maximum power of 13.69 watts at 194 rpm when the load is 1.5 kg. This is followed by a 75% baffle turbine, which reaches its maximum power of 11.03 watts at 150 rpm at a load of 1.75 kg. Turbines with no baffles and 25% baffles display a similar trend to the 50% baffle turbine, reaching their maximum power at a 1.5 kg load - 10.88 watts at 195 rpm for the no-baffle turbine, and 10.78 watts at 184 rpm for the 25% baffle turbine. The smallest maximum power among the baffle variations is 10.06 watts at 145 rpm, observed in the 100% baffle turbine at a 1.75 kg load. Of the 5 baffle variations, the turbines with no baffles, 25% baffles, and 50% baffles exhibit a similar power curve that peaks at a 1.5 kg load, while the 75% and 100% baffles reach their maximum power at lower speeds when the load is 1.75 kg. The power generated is influenced by the addition of a baffle plate that functions to hold water which can increase torque. The increase in torque will also increase the mechanical power.

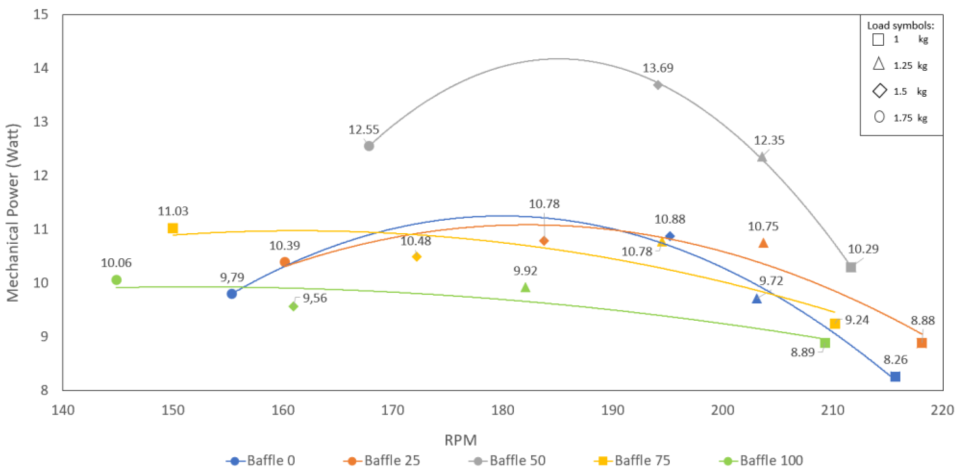

Figure 8. Stage 1 Mechanical Power

Figure 9 presents the results of the stage 2 mechanical power when paired with 5 variations of the stage 1 turbines. In this test, the stage 2 turbine had a constant load of 1 kg. The stage 2 turbine produces the highest mechanical power of 5.46 watts at 114 rpm when paired with a stage 1 turbine with a 50% baffle variation and a 1.75 kg load. When paired with a stage 1 turbine variation without baffles, 25% baffle, and 50% baffle, the difference in speed and power on stage 2 is not very significant when stage 1 is still under a load of 1-1.5 kg. However, a significant difference is observed in the yield power of stage 2 when paired with stage 1 using 75% and 100% baffles, where the power decreases as the load on stage 1 increases. The graph shows that when paired with stage 1 with a 75% baffle, the maximum power produced only reaches 4.31 watts at 126 rpm. When paired with stage 1 using a 100% baffle, the maximum power is lower, at 3.97 watts at 132 rpm. This significant decrease is caused when stage 1 with a 75% baffle and 100% vortex height drops dramatically, causing the vortex air core to increase in size, resulting in less water contact with the stage 2 turbine.

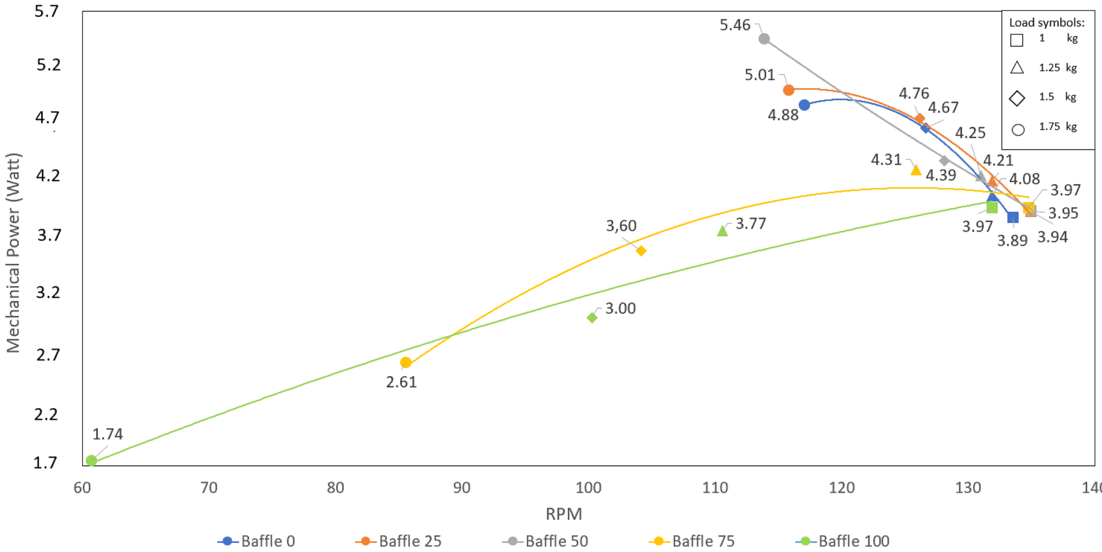

Figure 9. Stage 2 Mechanical Power

The total power of all the stages has an effect on each other. The stage 1 turbine with a 50% baffle variation produces the most total power across all variations and load conditions, with a maximum total power of 18.08 watts. Figure 10 shows the total power produced by the two-stage GWVT with different baffle plate variations on the first stage.

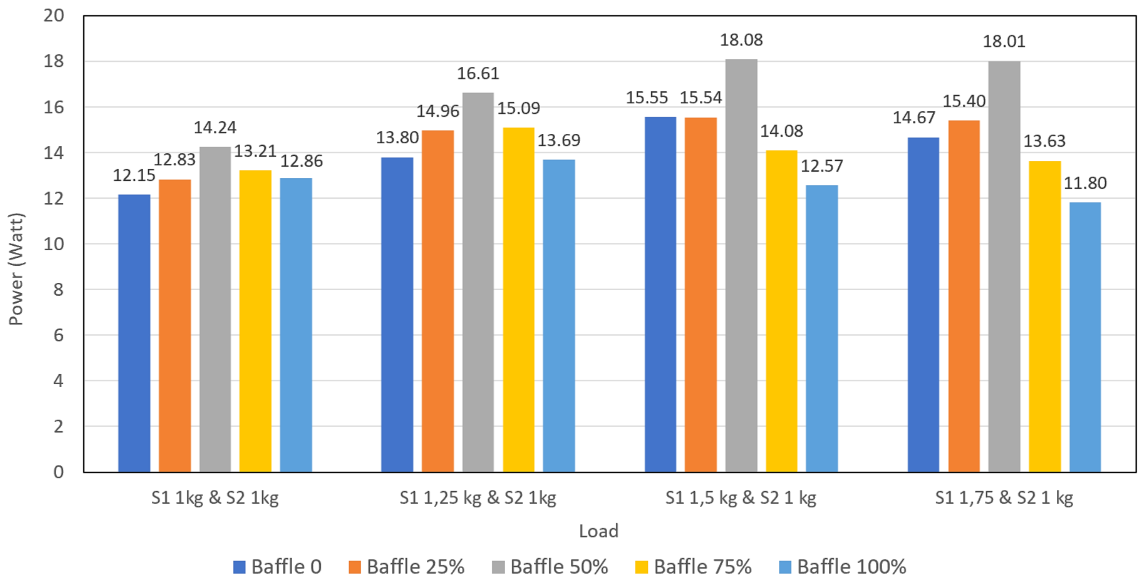

Figure 10. Total Power of Double-stage GWVT

3.3. Efficiency

Turbine efficiency is the ratio between the mechanical power produced and the power input. Efficiency demonstrates how optimally the turbine converts the available energy from water into usable power output.

Figure 11 shows the efficiency generated by the stage 1 turbine. Turbines without baffles have the highest efficiency, reaching 13.65% at 195 rpm, although this drops to 12.44% at 155 rpm. Turbines with 25% baffles achieve a slightly higher maximum efficiency of 13.69% at 184 rpm. The 50% baffle turbine reaches the highest overall efficiency, peaking at 16.79% at 194 rpm with a 1.5 kg load, before declining to 16.13% at 168 rpm with a 1.75 kg load. In contrast, the 75% baffle turbine has a maximum efficiency of 14.70% at 150 rpm when loaded with 1.75 kg, while the 100% baffle turbine reaches 14.11% at 145 rpm with the same 1.75 kg load.

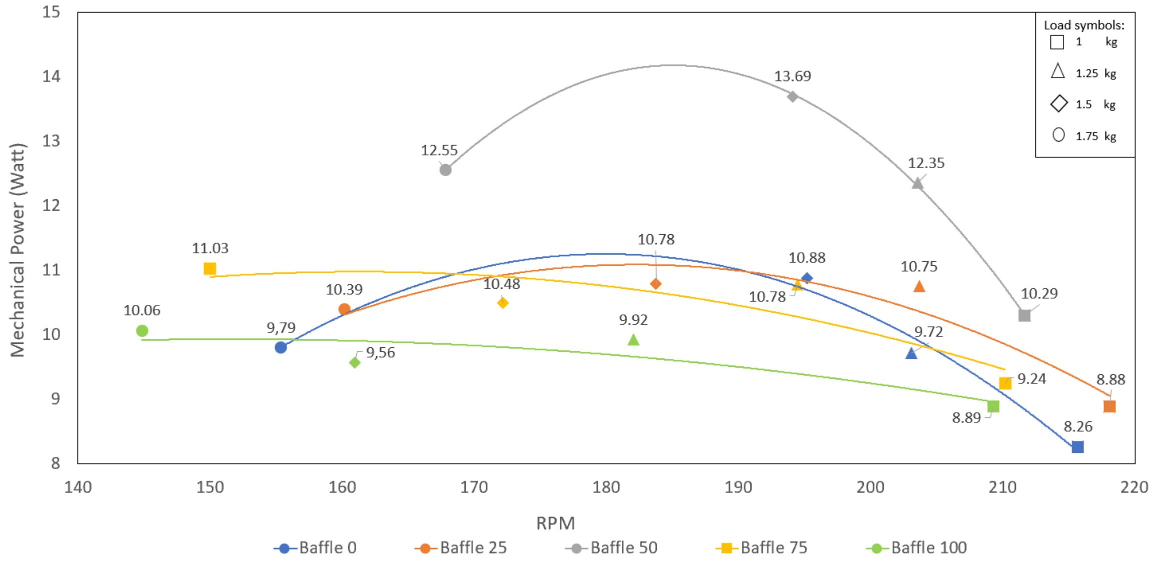

Figure 11. Stage 1 Efficiency

The graph in Figure 12 shows the efficiency of the stage 2 turbine when paired with different variations of the stage 1 turbine. The 75% and 100% baffle turbines exhibit the same trend as shown in Figure 9, with the efficiency decreasing as the load on the stage 1 turbine increases. When paired with a 100% baffle turbine, the maximum efficiency reaches only 4.71% at 132 rpm. Similarly, when paired with a 75% baffle turbine, the highest efficiency is 5.28% at 126 rpm. In contrast, the maximum efficiency when paired with 50% baffles reaches 7.02% at 114 rpm, which is the highest efficiency of stage 2 compared to the other stage 1 variations. When paired with a 25% baffle, the maximum efficiency reaches 6.33% at 116 rpm, while for turbines with no baffle, the maximum efficiency is slightly lower at 6.19% at 117 rpm.

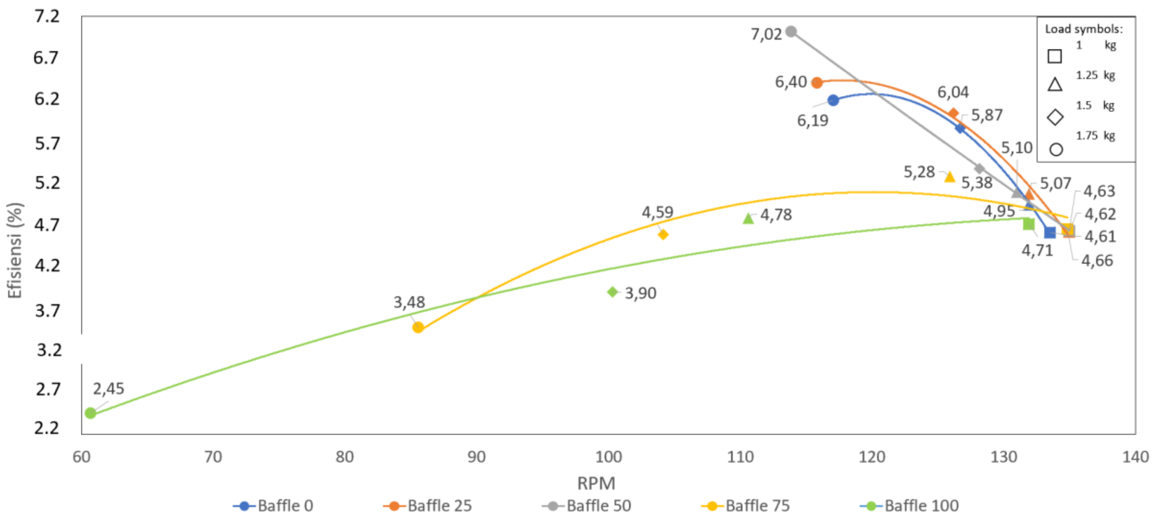

Figure 12. Stage 2 Efficiency

The total efficiency of each baffle variation at Stage 1 is shown in Figure 13. The double-stage GWVT turbine reaches its maximum total efficiency of 23.15% when Stage 1 with a 50% baffle variation at 1.75 kg load is combined with the Stage 2 turbine at 1 kg load. The Stage 1 turbine with a 50% baffle is the most efficient combination across all loadings. In contrast, when the Stage 1 turbine uses no baffles, its highest overall efficiency is only 19.52%. This demonstrates that the addition of a 50% baffle can increase the efficiency of the two-stage GWVT by 3.63%.

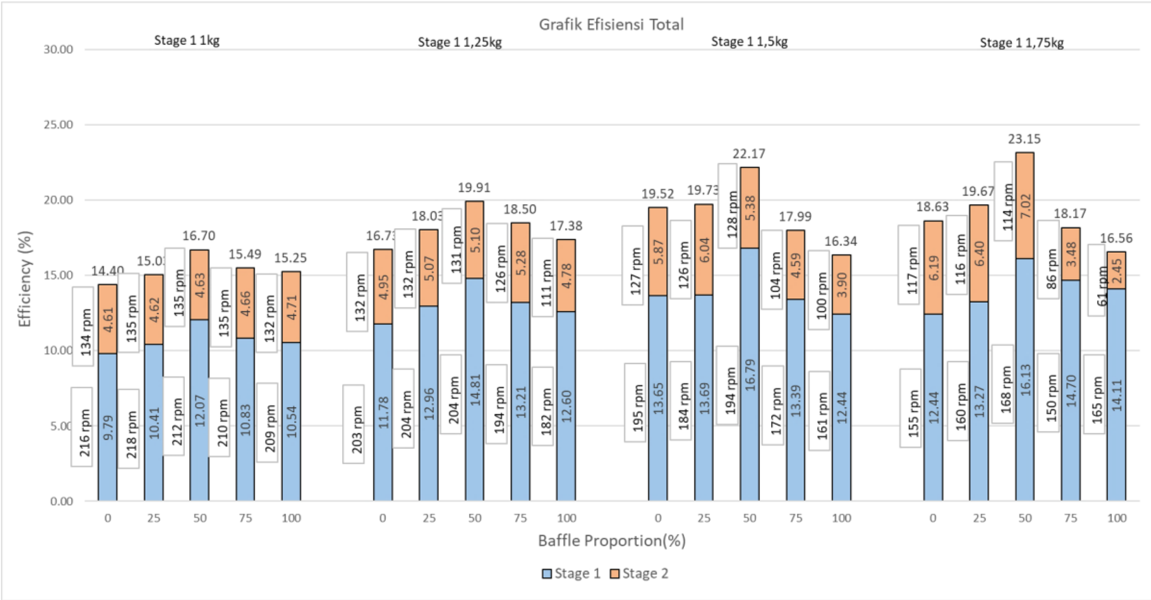

Figure 13. Total Efficiency

3.4. Research Comparison

Vortex turbines are micro-pico hydro scale turbines that work with an average head of 0.7 - 2 m [33]. In comparison with several other types of turbines, the vortex turbine's efficiency is approximately 30–35% higher than the Savonius turbine [14]. This is significantly lower than the efficiency performance of the Francis turbine [53], around 93%, and the Kaplan turbine [54], which ranges from 87% to 90%. However, vortex turbines offer significant advantages for application, such as uncomplicated construction, ease of maintenance, and cost-effectiveness for installation in low-head areas [52]. In practical application, vortex turbines necessitate the selection of suitable materials to ensure an extended lifetime of use. Sritam's study indicates that Al turbines outperform Fe turbines in performance [11]. While turbines made of light materials have better-starting torsion, using denser materials in the flywheel energy storage system makes the kinetic energy much more stable during rotation, especially when a lot of power is needed [55]. Its baffle structure indirectly augments the turbine's weight, hence enabling its commercial application to achieve a substantial flywheel effect. The research undertaken is a laboratory-scale experiment with notably low-efficiency values, ranging from 14.40% to 23.50%. Table 3 presents a comparative analysis of prior research alongside the double-stage baffle vortex turbine study.

Table 3. The comparison of the present study to earlier vortex turbine studies

Ref.	Variations	Configuration	Performance
[56]	The Baffle Plate effect with varying top, bottom, double, and no baffle configurations.	Single-stage	• Without: 25.22% • Top Baffle: 22.21% • Bottom Baffle: 32.33% • Double Baffle: 32.39%
[44]	Effect of baffle proportion 0%, 25%, 50%, 75%, and 100%	Single-stage	The best ratio is 50%, with 32.79% efficiency and torque of 37.41 Nm.
Present study	Effect of baffle proportion %, 25%, 50%, 75%, and 100% on two-stage vortex turbine configuration at constant flow rate and loading rate	Double-stage	The best baffle configuration is achieved at a flow rate of 9.5 L/s by a proportion of 50% baffles with the most significant output of 18.08 W at a load of 1.5 kg
[57]	Effects of runner diameter ratio (RB) and installation position	Three-Stage	The runner with RB=0.6, located near the outlet basin, has an efficiency of approximately 80%.
[34]	Testing vortex turbines with single-stage, two-stage, and three-stage configurations	Multi-stage	Inter-stage increases in torque: 0.27 Nm, 0.41 Nm, 0.44 Nm.

3.5. Statistical Analysis

This double-stage turbine experiment uses a constant flow rate and the same S2 configuration; therefore, confounding factors like turbulence vortex flow are not detail considered and are assumed to be a research limitation. Based on the earlier works, the fluid's flow structure is uniform since entering the basin and changes after being extracted by the turbine [33]. Correspondingly, the fundamental assumption of fluid flow characteristics after harnessing by S2 is uniform because of its same geometrical configurations along the different S1 blade proportions. Co-axial flow caused by the S2 turbine is the fundamental idea behind developing the baffle to harness the available flow characteristic within the basin and maximize efficiency. Since the confidence interval is 5%, the P_{total} between S1 and S2 for all configurations is evaluated using a double-factor variance analysis (provided in Table 4). It is found that the baffle variable has a significant influence on the double-stage vortex turbine's performance since the result of the P-value (0.02) is less than 0.05. If we look more closely at Table 4, the P-value load also significantly influences the turbine's performance; thus, we can use Equation 6 to get the effective contribution (SE). According to the linear regression statistical analysis, the $r_{cor\text{-}load}$ is 0.289, and the $r_{cor\text{-}Baffle}$ is 0.344, whereas the β_{load} and β_{Baffle} values were 0.272 and 0.357, respectively. The results for the effective contribution between load and baffle are 12.28% and 7.86%, respectively. That's even more than 79.86%, an undefined variable that highly influences the working vortex turbine. Based on the literature, it can be the effect of vorticity and flow characteristics [17]. In conclusion, the baffle proportion plays a crucial role in this study, demonstrating a notable impact of 7.86% under constant flow rate conditions, while a 50% baffle proportion represents an optimal power output of 23.15 Watt.

$$SE(X) = \beta_x \times r_{cor-x} \times 100\% \quad (6)$$

Table 4. Analysis of Variance

P-total	*SS*	*df*	*MS*	*F*	*P-value*	*F crit*
Baffle Portion	13.29124	3	4.430413	4.720398	0.021256	3.490295
Load	34.40004	4	8.60001	9.162909	0.001243	3.259167
Error	11.26281	12	0.938568			
Total	58.95409	19				

Statistical analysis of experimental data is highly useful in confirming that the examined and analyzed data have an acceptable distribution from which to conclude. In this section, the turbine's torque, mechanical power, and efficiency data are analyzed and classified using variables, namely 0%, 25%, 50%, 75%, and 100% blade baffle proportion. The statistical study used the Mean Square Error (MSE) established by Coleman et al., in which the experimental data is compared to previously predicted data produced by the linear regression approach [52]. Equations 7, 8, and 9 show the revised formulas for MSE torque, mechanical power, and efficiency.

$$MAE_T = \frac{1}{N}\sum_1^N \left|T_{exp} - T_{Pred}\right| \quad (7)$$

$$MAE_{Pm} = \frac{1}{N}\sum_1^N \left|P_{exp} - Pm_{Pred}\right| \quad (8)$$

$$MAE_\eta = \frac{1}{N}\sum_1^N \left|\eta_{exp} - \eta_{Pred}\right| \quad (9)$$

Figure 14 depicts the MSE analysis results for comparing the distribution of experimental data to predicted data. The prediction data used is derived from the standardized prediction of the statistical linear regression test findings in Equations 10 to 12, where X1 represents the prony brake load variation and X2 represents the baffle blade proportion variable. The distribution of experimental data has a good match, with no more than ±10% data error. This allows for the comparison of results and conclusions.

$$T_{Pred} = 0.0678X_1 + 0.3250X_2 + 0.0005 \quad (10)$$

$$Pm_{Pred} = 2.7337X_1 + 0.2466X_2 + 0.0196 \quad (11)$$

$$\eta_{Pred} = 4.4453X_1 + 0.0058X_2 + 6.6751 \quad (12)$$

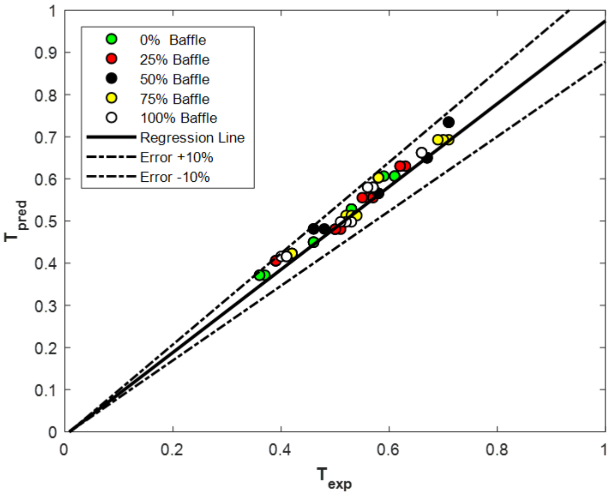

(a)

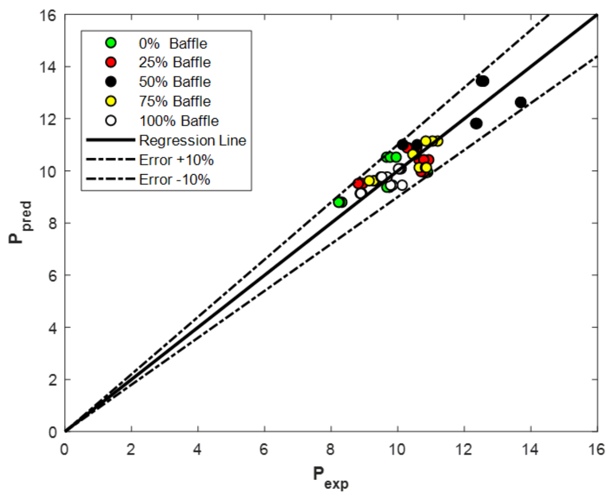

(b)

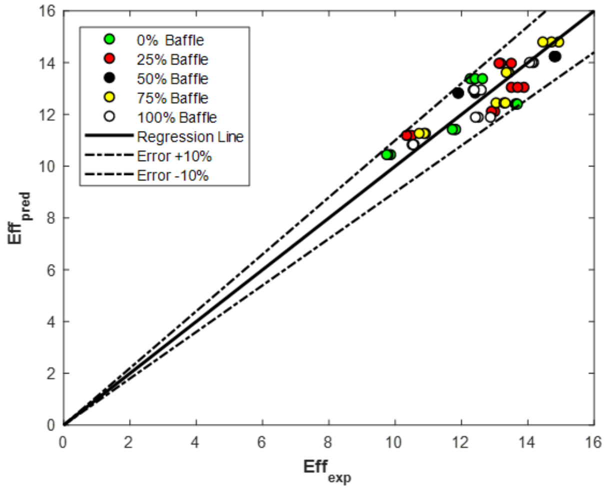

(c)

Figure 14. Distribution of MSE data from experimental results compared to predicted data for (a) Torque, (b) Mechanical power, and (c) Efficiency

The analysis indicates that a double-factor variance analysis test, conducted with a 5% confidence interval, reveals a significant impact of baffle proportions. Additionally, the data collected during the experiment exhibits a ±10% error margin. The acceptability of this interval distribution error is notably high, particularly in experimental areas. To strengthen our argument, we analyzed the propagation error of the 0% baffle data sample at each loading variation. The data collected at each load, along with the proportion of baffles, can be defined from each data collection. A significant propagation error (PE) can be determined and calculated using the formula. $PE = \sqrt{\Delta B^2 + \Delta R^2}$. The error of the experiment can consist of bias (ΔB) and random error (ΔR). The calculation of bias ΔB relies on the precision of the measuring instruments, specifically the load cell and tachometer, which have accuracies of 0.01 and 0.01 respectively. The calculation of random errors in load and RPM data collection is expressed as $\Delta R = \sigma \times (t/df)$ where σ represents the standard deviation, t denotes the t-table value, and df indicates the degree of freedom. The simultaneous formulas for ΔB_T and ΔR_T are presented in Equations 13 and 14, where r represents the radius of the turbine. Meanwhile, ΔB_P and ΔR_P are determined using Equations 15 and 16. The analysis of propagation error indicates that the error intervals for load, RPM, T (Torque), and P (Power) data are 2.39%, 0.41%, 0.75%, and 9.67%, respectively. The results align with the MSE prediction data distribution, approximately within a maximum range of 10% (Table 5).

$$\Delta B_T = \sqrt{(r \times \Delta B_{load})^2} \tag{13}$$

$$\Delta R_T = \sqrt{(r + \Delta R_{load})^2} \tag{14}$$

$$\Delta B_P = \sqrt{(\Delta P \times \Delta B_T)^2 + (\Delta P \times \Delta B_{RPM})^2} \tag{15}$$

$$\Delta R_P = \sqrt{(\Delta P \times \Delta R_T)^2 + (\Delta P \times \Delta R_{RPM})^2} \tag{16}$$

Table 5. Uncertainty Analysis

Parameters	F (Load)	T	RPM	P
Mean	13.30	0.37	22.58	8.26
Standard Deviation	0.072	0.002	0.021	0.051
n-data	3	3	3	3
df	2	2	2	2
Cl	95%	95%	95%	95%
α	5%	5%	5%	5%
ΔR	0.010	0.009	0.010	0.112
t-table	6.21		6.21	
ΔB	0.317	0.029	0.091	0.791
PE	0.317	0.003	0.092	0.799
Error Estimation	2.39%	0.75%	0.41%	9.67%

4. Conclusion

Experimental analyses on using baffle plates in a double-stage vortex turbine with varied loads have been completed. The results elaborate that installing baffle plates in stage 1 influences the total power output. It is concluded that the best baffle configuration is achieved at a flow rate of 9.5 L/s by a proportion of 50% baffles with the most significant output of 18.08 W at a load of 1.5 kg. The data obtained varies and has a small gap; therefore, we conducted statistical analysis to confirm that baffle proportion has a significant effect. The considerable effect of the baffle is supported by the result of MSE with the margin range data error of ±10% between experimental data and predicted data. The propagation error also shows that the confidence interval and margin error for the measurements of load, RPM, torque, and mechanical power are 2.39%, 0.41%, 0.725%, and 9.67%, respectively. These results show that this research has a small error distribution and can be considered scientifically. Even the power and efficiency are still relatively small because this research is done on a laboratory scale with a radius of 91 mm. These laboratory-scale results hold promising potential for application in larger-scale conditions. The experiments have not described the fluid flow characteristics in the basin, which limits this research. Therefore, this research has great potential for further development through numerical computational and software-based simulations to obtain detailed and fundamental vortex flow characteristics.

5. Declarations

5.1. Author Contributions

Conceptualization, A.P., M.D.S., and S.H.; methodology, A.P., R.M., and S.H.; software, E.P.B. and D.M.P.; validation, M.D.S., E.P.B., and A.P.; formal analysis, A.P., R.M., M.D.S., and S.H.; investigation, A.P., R.M., M.D.S., and S.H.; resources, A.P., M.D.S., and S.H.; data curation, A.P., E.P.B. and D.M.S..; writing—original draft preparation, A.P., D.A., M.D.S., and S.H.; writing—review and editing, A.P., D.A., R.M., M.D.S., and S.H..; visualization, A.P., M.D., and M.D.S.; supervision, A.P., M.D.S., and S.H.; project administration, A.P., R.M., and M.D.S.; funding acquisition, A.P., M.D.S., and S.H. All authors have read and agreed to the published version of the manuscript.

5.2. Data Availability Statement

The data presented in this study are available on request from the corresponding author.

5.3. Funding and Acknowledgments

This work was supported by the RKAT PTNBH Universitas Sebelas Maret Year 2023, under the Research Scheme of "Penelitian Unggulan Terapan" (PUT-UNS), with research grant/contract no. 228/UN27.22/PT.01.03/2023. The support is gratefully acknowledged by the authors.

5.4. Conflicts of Interest

The authors declare no conflict of interest.

6. References

[1] International Energy Agency. (2022). World energy outlook 2022. International Energy Agency, Paris, France. doi:10.1787/3a469970-en.

[2] Suryatna, B. S., Agustina, T., & Sugiarto. (2021). Prototype design of waterwheel micro hydro power plants for small water discharge. IOP Conference Series: Earth and Environmental Science, 700(1), 12032. doi:10.1088/1755-1315/700/1/012032.

[3] BPPT. (2021). Outlook Energi Indonesia 2021. National Energy Council of the Republic of Indonesia, Jakarta, Indonesia. Available online: https://www.den.go.id/publikasi/Outlook-Energi-Indonesia (accessed on January 2025).

[4] U.S. Department of Energy (2025). Benefits of Hydropower. Committed to Restoring America's Energy Dominance, Washington, United States. Available online: https://www.energy.gov/eere/water/benefits-hydropower (accessed on January 2025).

[5] Kaunda, C. S., Kimambo, C. Z., & Nielsen, T. K. (2012). Hydropower in the Context of Sustainable Energy Supply: A Review of Technologies and Challenges. ISRN Renewable Energy, 2012, 1–15. doi:10.5402/2012/730631.

[6] Kunalan, K. T. (2022). A performance investigation of a multi-staging hydrokinetic turbine for river flow. Progress in Energy and Environment, 17(1), 17–31. doi:10.37934/progee.17.1.1731.

[7] Williamson, S. J., Stark, B. H., & Booker, J. D. (2013). Performance of a low-head pico-hydro Turgo turbine. Applied Energy, 102, 1114–1126. doi:10.1016/j.apenergy.2012.06.029.

[8] Arfoa, A., Al-Mashakbeh, S., Al-Mashakbeh, A. S., & Awwad, A. E. (2023). Design and Analysis of a Fish-Friendly Micro Gravitational Water Vortex Power Plant (GWVPP) on Zarqa River, Jordan. Indonesian Journal of Electrical Engineering and Informatics, 11(2), 469-484. doi:10.52549/.v11i2.4382.

[9] Prabowoputra, D. M. (2022). Simulation Study on Cross Flow Turbine Performance with an Angle of 20° to the Variation of the Number of Blades. International Journal of Mechanical Engineering and Robotics Research, 11(1), 31–36. doi:10.18178/ijmerr.11.1.31-36.

[10] Mobeen, M., Jaweed, S., Abdullah, A., Rasheed, S., & Masud, M. (2023). Parametric Optimization of Gravitational Water Vortex Turbines for Enhanced Torque Generation †. Engineering Proceedings, 45(1), 3. doi:10.3390/engproc2023045003.

[11] Sritram, P., Treedet, W., & Suntivarakorn, R. (2015). Effect of turbine materials on power generation efficiency from free water vortex hydro power plant. IOP Conference Series: Materials Science and Engineering, 103(1), 12018. doi:10.1088/1757-899X/103/1/012018.

[12] Dhakal, S., Timilsina, A. B., Dhakal, R., Fuyal, D., Bajracharya, T. R., Pandit, H. P., Amatya, N., & Nakarmi, A. M. (2015). Comparison of cylindrical and conical basins with optimum position of runner: Gravitational water vortex power plant. Renewable and Sustainable Energy Reviews, 48, 662–669. doi:10.1016/j.rser.2015.04.030.

[13] Nishi, Y., & Inagaki, T. (2017). Performance and Flow Field of a Gravitation Vortex Type Water Turbine. International Journal of Rotating Machinery, 2017, 1–11. doi:10.1155/2017/2610508.

[14] Timilsina, A. B., Mulligan, S., & Bajracharya, T. R. (2018). Water vortex hydropower technology: a state-of-the-art review of developmental trends. Clean Technologies and Environmental Policy, 20(8), 1737–1760. doi:10.1007/s10098-018-1589-0.

[15] Khan, T., Asif, M. M., Ahmed, H., Islam, M., & Harun, Z. (2021). Design and Development of a Vortex Turbine for the Hilly Regions of Bangladesh. Proceedings of the 2nd International Seminar of Science and Applied Technology (ISSAT 2021), 290-297. doi:10.2991/aer.k.211106.046.

[16] Handoko, R., Septiyanto, M. D., Tjahjana, D. D. D. P., Himawanto, D. A., Yaningsih, I., & Hadi, S. (2023). Performance Testing and Analysis of Gravitational Water Vortex Turbine: A Modified Experimental Study on Blade Arc and Inclination Angle. Journal of Advanced Research in Fluid Mechanics and Thermal Sciences, 109(1), 147–161. doi:10.37934/arfmts.109.1.147161.

[17] Rahman, M. M., Tan, J. H., Fadzlita, M. T., & Wan Khairul Muzammil, A. R. (2017). A Review on the Development of Gravitational Water Vortex Power Plant as Alternative Renewable Energy Resources. IOP Conference Series: Materials Science and Engineering, 217(1), 12007. doi:10.1088/1757-899X/217/1/012007.

[18] Maulana, D. W., Rizwan, F. M., Mulyana, C., Faizal, F., Panatarani, C., & Joni, I. M. (2020). Gravitational water vortex Pico hydro power modeling for aquaculture implementation. Journal of Physics: Conference Series, 1568(1), 12016. doi:10.1088/1742-6596/1568/1/012016.

[19] Bajracharya, T. R., Shakya, S. R., Timilsina, A. B., Dhakal, J., Neupane, S., Gautam, A., & Sapkota, A. (2020). Effects of Geometrical Parameters in Gravitational Water Vortex Turbines with Conical Basin. Journal of Renewable Energy, 2020, 1–16. doi:10.1155/2020/5373784.

[20] Nishi, Y., Suzuo, R., Sukemori, D., & Inagaki, T. (2020). Loss analysis of gravitation vortex type water turbine and influence of flow rate on the turbine's performance. Renewable Energy, 155, 1103–1117. doi:10.1016/j.renene.2020.03.186.

[21] Saleem, A. S., Cheema, T. A., Ullah, R., Ahmad, S. M., Chattha, J. A., Akbar, B., & Park, C. W. (2020). Parametric study of single-stage gravitational water vortex turbine with cylindrical basin. Energy, 200, 117464. doi:10.1016/j.energy.2020.117464.

[22] Srihari, P. S. V. V., Narayana, P. S. V. V. S., Kumar, K. V. V. S. S., Raju, G. J., Naveen, K., & Anand, P. (2019). Experimental study on vortex intensification of gravitational water vortex turbine with novel conical basin. 1ST International Conference on Manufacturing, Material Science and Engineering (ICMMSE-2019), 2200, 020082. doi:10.1063/1.5141252.

[23] Chattha, J. A., Cheema, T. A., & Khan, N. H. (2017). Numerical investigation of basin geometries for vortex generation in a gravitational water vortex power plant. 2017 8th International Renewable Energy Congress (IREC), 1–5. doi:10.1109/irec.2017.7926028.

[24] Rostami, A. B., & Armandei, M. (2017). Renewable energy harvesting by vortex-induced motions: Review and benchmarking of technologies. Renewable and Sustainable Energy Reviews, 70, 193–214. doi:10.1016/j.rser.2016.11.202.

[25] Sotoudeh, N., Maddahian, R., & Cervantes, M. J. (2019). Formation of Rotating Vortex Rope in the Francis-99 Draft Tube. IOP Conference Series: Earth and Environmental Science, 240, 022017. doi:10.1088/1755-1315/240/2/022017.

[26] Payambarpour, S. A., Najafi, A. F., & Magagnato, F. (2019). Investigation of Blade Number Effect on Hydraulic Performance of In-Pipe Hydro Savonius Turbine. International Journal of Rotating Machinery, 2019, 1–14. doi:10.1155/2019/8394191.

[27] Kueh, T. C., Beh, S. L., Ooi, Y. S., & Rilling, D. G. (2017). Experimental study to the influences of rotational speed and blade shape on water vortex turbine performance. Journal of Physics: Conference Series, 822(1), 12066. doi:10.1088/1742-6596/822/1/012066.

[28] Adeyeye, K. A., Ijumba, N., & Colton, J. (2021). The Effect of the Number of Blades on the Efficiency of a Wind Turbine. IOP Conference Series: Earth and Environmental Science, 801(1), 012020. doi:10.1088/1755-1315/801/1/012020.

[29] Zhou, G., & Ye, Q. (2012). Experimental investigations of thermal and flow characteristics of curved trapezoidal winglet type vortex generators. Applied Thermal Engineering, 37, 241–248. doi:10.1016/j.applthermaleng.2011.11.024.

[30] Zhang, L. J., Xie, M. P., & Li, Y. P. (2018). Analysis on hydraulic characteristics of Kaplan water turbine with different spiral casing and stay vane. IOP Conference Series: Earth and Environmental Science, 163(1), 12063. doi:10.1088/1755-1315/163/1/012063.

[31] Yaakob, O. B., M. Ahmed, Y., Elbatran, A. H., & Shabara, H. M. (2014). A Review on Micro Hydro Gravitational Vortex Power and Turbine Systems. Jurnal Teknologi, 69(7), 1-7. doi:10.11113/jt.v69.3259.

[32] Shrestha, U., Chen, Z., & Choi, Y. Do. (2018). Study on the effect of the runner design parameters on 50 MW Francis hydro turbine model performance. Journal of Physics: Conference Series, 1042(1), 12006. doi:10.1088/1742-6596/1042/1/012006.

[33] Ullah, R., Cheema, T. A., Saleem, A. S., Ahmad, S. M., Chattha, J. A., & Park, C. W. (2019). Performance analysis of multi-stage gravitational water vortex turbine. Energy Conversion and Management, 198, 111788. doi:10.1016/j.enconman.2019.111788.

[34] Cheema, T. A., Ullah, R., & Saleem, A. S. (2019). Performance analysis of a two-stage gravitational water vortex turbine. IOP Conference Series: Earth and Environmental Science, 291(1), 12039. doi:10.1088/1755-1315/291/1/012039.

[35] Zhao, R., Zhuge, W., Zhang, Y., Yang, M., Martinez-Botas, R., & Yin, Y. (2015). Study of two-stage turbine characteristic and its influence on turbo-compound engine performance. Energy Conversion and Management, 95, 414–423. doi:10.1016/j.enconman.2015.01.079.

[36] Kayastha, M., Raut, P., Subedi, N. K., Ghising, S. T., & Dhakal, R. (2019). CFD evaluation of performance of Gravitational Water Vortex Turbine at different runner positions. KECConference2019, Kantipur Engineering College, Dhapakhel, Lalitpur, Nepal. doi:10.31224/osf.io/d9qn3.

[37] Wanchat, S., Suntivarakorn, R., Wanchat, S., Tonmit, K., & Kayanyiem, P. (2013). A parametric study of a gravitation vortex power plant. Advanced Materials Research, 805–806, 811–817. doi:10.4028/www.scientific.net/AMR.805-806.811.

[38] Aziz, M. Q. A., Idris, J., & Abdullah, M. F. (2022). Experimental Study on Enclosed Gravitational Water Vortex Turbine (GWVT) Producing Optimum Power Output for Energy Production. Journal of Advanced Research in Fluid Mechanics and Thermal Sciences, 95(2), 146–158. doi:10.37934/arfmts.95.2.146158.

[39] Dahal, N., Shrestha, R. K., Sherchan, S., Milapati, S., Shakya, S. R., & Jha, A. K. (2020). Performance Analysis of Booster based Gravitational Water Vortex Power Plant. Journal of the Institute of Engineering, 15(3), 90–96. doi:10.3126/jie.v15i3.32026.

[40] Nadhief, M. I., Prabowoputra, D. M., Hadi, S., & Tjahjana, D. D. D. P. (2020). Experimental study on the effect of variation of blade arc angle to the performance of savonius water turbine flow in pipe. International Journal of Mechanical Engineering and Robotics Research, 9(5), 779–783. doi:10.18178/ijmerr.9.5.779-783.

[41] Prasetyo, H., Budiana, E. P., Tjahjana, D., & Hadi, S. (2018). The Simulation Study of Horizontal Axis Water Turbine Using Flow Simulation Solidworks Application. IOP Conference Series: Materials Science and Engineering, 308(1), 12022. doi:10.1088/1757-899X/308/1/012022.

[42] Mulligan, S., De Cesare, G., Casserly, J., & Sherlock, R. (2018). Understanding turbulent free-surface vortex flows using a Taylor-Couette flow analogy. Scientific Reports, 8(1), 824. doi:10.1038/s41598-017-16950-w.

[43] Sritram, P., & Suntivarakorn, R. (2019). The effects of blade number and turbine baffle plates on the efficiency of free-vortex water turbines. IOP Conference Series: Earth and Environmental Science, 257(1), 12040. doi:10.1088/1755-1315/257/1/012040.

[44] Wichian, P., & Suntivarakorn, R. (2016). The Effects of Turbine Baffle Plates on the Efficiency of Water Free Vortex Turbines. Energy Procedia, 100, 198–202. doi:10.1016/j.egypro.2016.10.165.

[45] Chen, L., Chen, J., & Zhang, Z. (2018). Review of the Savonius rotor's blade profile and its performance. Journal of Renewable and Sustainable Energy, 10(1), 013306. doi:10.1063/1.5012024.

[46] Prabowoputra, D. M., & Prabowo, A. R. (2022). Effect of Geometry Modification on Turbine Performance: Mini-Review of Savonius Rotor. International Journal of Mechanical Engineering and Robotics Research, 11(10), 777–783. doi:10.18178/ijmerr.11.10.777-783.

[47] Jeon, K. S., Jeong, J. I., Pan, J. K., & Ryu, K. W. (2015). Effects of end plates with various shapes and sizes on helical Savonius wind turbines. Renewable Energy, 79(1), 167–176. doi:10.1016/j.renene.2014.11.035.

[48] Kassab, S. Z., Chemengich, S. J., & Lotfy, E. R. (2022). The effect of endplate addition on the performance of the savonius wind turbine: A 3-D study. Proceedings of the Institution of Mechanical Engineers, Part A: Journal of Power and Energy, 236(8), 1582–1592. doi:10.1177/09576509221098480.

[49] Dhakal, R., Bajracharya, T. R., Shakya, S. R., Kumal, B., Kathmandu, N., Khanal, K., Kavre, N., Williamson, S. J., Gautam, S., & Ghale, D. P. (2017). Computational and experimental investigation of runner for gravitational water vortex power plant. Proceedings of a Meeting Held, 5, 8. doi:10.31219/osf.io/4r5cj.

[50] Septyaningrum, E., Sutardi, S., Hantoro, R., Rijal Firdausi, A., & Prasetyo, R. A. (2024). The effect of runner installation and design on the performance of gravitational vortex water turbine. International Journal of Green Energy, 21(7), 1434-1446. doi:10.1080/15435075.2023.2253900.

[51] Sinaga, D. A., Septiyanto, M. D., Arifin, Z., Rusdiyanto, G., Prasetyo, S. D., & Hadi, S. (2023). The Effect of Blade Distances on the Performance of Double-Stage Gravitational Water Vortex Turbine. Journal of Advanced Research in Fluid Mechanics and Thermal Sciences, 109(1), 196–209. doi:10.37934/arfmts.109.1.196209.

[52] Coleman, H. W., & Steele, W. G. (2009). Experimentation, Validation, and Uncertainty Analysis for Engineers. John Wiley & Sons, Hoboken, United States. doi:10.1002/9780470485682.

[53] Trivedi, C., Cervantes, M. J., & Dahlhaug, O. G. (2016). Experimental and numerical studies of a high-head Francis turbine: A review of the Francis-99 test case. Energies, 9(2), 74. doi:10.3390/en9020074.

[54] Krzemianowski, Z., & Kaniecki, M. (2023). Low-head high specific speed Kaplan turbine for small hydropower – design, CFD loss analysis and basic, cavitation and runaway investigations: A case study. Energy Conversion and Management, 276, 116558. doi:10.1016/j.enconman.2022.116558.

[55] Li, X., & Palazzolo, A. (2022). A review of flywheel energy storage systems: state of the art and opportunities. Journal of Energy Storage, 46, 103576. doi:10.1016/j.est.2021.103576.

[56] Rahman, R. A., Septiyanto, M. D., Prasetyo, A., Kristiawan, B., Adrianto, S., & Hadi, S. (2024). The effect of the additional baffle plate on vortex turbine performance. AIP Conference Proceedings, 3069(1), 20017. doi:10.1063/5.0205754.

[57] Ullah, R., & Cheema, T. A. (2022). Experimental Investigation of Runner Design Parameters on the Performance of Vortex Turbine. Engineering Proceedings, 23(1), 14. doi:10.3390/engproc2022023014.